



Alkaline zirconates as effective materials for hydrogen production through consecutive carbon dioxide capture and conversion in methane dry reforming

J. Arturo Mendoza-Nieto^{a,*}, Yuhua Duan^b, Heriberto Pfeiffer^c

^a Facultad de Química, Departamento de Fisicoquímica, Universidad Nacional Autónoma de México, Ciudad Universitaria, Del. Coyoacán, CP 04510, Ciudad de México, Mexico

^b National Energy Technology Laboratory, United States Department of Energy, 626 Cochran Mill Road, Pittsburgh, PA, 15236, United States

^c Laboratorio de Fisicoquímica y Reactividad de Superficies (LaFReS), Instituto de Investigaciones en Materiales, Universidad Nacional Autónoma de México, Circuito exterior s/n, Ciudad Universitaria, Del. Coyoacán, CP 04510, Ciudad de México, Mexico



ARTICLE INFO

Keywords:

Dry CH₄ reforming
CO₂ chemisorption
Lithium zirconate
Sodium zirconate
CO oxidation

ABSTRACT

In this work, H₂ production was evaluated using different carbonation conditions and two alkaline zirconates. For this purpose, Li₂ZrO₃ and Na₂ZrO₃ were synthesized, characterized and tested on a consecutive process composed of initial CO₂ capture, followed by methane dry reforming (MDR). Thermogravimetric results showed that under the four gas mixtures tested (diluted and saturated CO₂, CO and CO-O₂), both ceramics are able to chemisorb CO₂, with Na₂ZrO₃ having the highest capture with saturated CO₂. In catalytic tests, ceramics carbonated with saturated CO₂ or CO-O₂ gas flows were able to act as sorbents and catalysts, producing H₂ at T > 750 °C through the partial oxidation of methane. This reaction was produced because CO₂ desorption did not occur, thus avoiding the MDR process. On the other hand, carbonated ceramics under a CO-O₂ gas mixture presented an outstanding catalytic performance. Between 450 and 750 °C, H₂ was formed through the MDR process promoted by CO₂ desorption from both ceramics. This result is in line with CO₂ desorption results, where a weaker CO₂-solid interaction was observed in comparison with saturated CO₂. Afterward, both ceramics presented a similar catalytic behavior, good regeneration and cyclability after the double process proposed (CO₂ capture-MDR reaction). Lithium zirconate also presented high thermal stability during cycle tests; meanwhile, sodium zirconate showed an important H₂ production increase as a function of cycles. Finally, both materials are feasible options for producing a clean energy source in a moderate temperature range through the catalytic conversion of two greenhouse gases (CO₂ and CH₄).

1. Introduction

Twenty years ago, Nakagawa and Ohashi [1] published the first report about CO₂ chemisorption on alkaline ceramics (lithium zirconate, Li₂ZrO₃) at high temperatures. Since then, several authors have reported many other alkaline ceramics as possible CO₂ chemisorbents, including sodium zirconate (Na₂ZrO₃) [2–5].

Focusing on lithium [1,6–9] and sodium [10–15] zirconates, the lithium version has a theoretical CO₂ capture capacity of 6.5 mmol of CO₂ per gram of ceramic (mmol_{CO2/g}), although it presents moderate CO₂ capture efficiency and kinetic properties between 400 and 600 °C. Accordingly, different studies have reported Li₂ZrO₃ structural or microstructural modifications to improve some of their CO₂ capture properties [7,16–18]. For example, Radfarnia and Iliuta [16]

synthesized porous Li₂ZrO₃ nanoparticles, producing microstructural changes. They observed better CO₂ sorption rates and efficiencies on porous nanopowders than those obtained with Li₂ZrO₃ prepared by traditional methods (solid-state reaction). On the other hand, Peltzer et al. [17] prepared K-doped Li₂ZrO₃, implying a chemical modification. In that case, a K-doped Li₂ZrO₃ sample presented significant CO₂ capture improvements with respect to undoped Li₂ZrO₃, even after 30 CO₂ sorption-desorption cycles. In contrast, Na₂ZrO₃ has a slightly lower theoretical CO₂ capture capacity (5.4 mmol CO₂/g) in comparison to lithium zirconate, but it presents higher CO₂ capture kinetics in a wide temperature range (250–800 °C) [15,19–21]. For example, a recent work published by Zhao et al. [20] showed that Na₂ZrO₃ has a rapid CO₂ sorption when it is prepared by the spray-dried method, enhancing CO₂ sorption-desorption cyclic stability.

* Corresponding author.

E-mail address: amendozan@comunidad.unam.mx (J.A. Mendoza-Nieto).

Moreover, in recent years, both zirconates and other alkaline ceramics have been proposed for different catalytic processes as catalysts or bifunctional materials [22–29]. Li_2ZrO_3 and Na_2ZrO_3 have been tested as possible basic heterogeneous catalysts for transesterification reactions of different molecules [25,26]. Recently, some alkaline zirconates have been used in the CO oxidation reaction, showing complete conversions to CO_2 between 450 and 600 °C and subsequent capture of CO_2 that was produced [30]. Correspondingly, among the possible bi-functionality of these ceramics, they have been tested as catalysts and CO_2 sorbents for different processes involving hydrogen production or purification [31–37]. For example, Zhao et al. [31] tested Na_2ZrO_3 as bifunctional catalyst-sorbent using cellulose as a biomass source under pyrolytic conditions, where Na_2ZrO_3 showed an important catalytic influence during pyrolysis catalyzing tar cracking and reforming reactions. Na_2ZrO_3 positively enhanced hydrogen production from cellulose, removing the CO_2 that was produced. In a different work, Wang et al. [35] described the use of Ni-based sorbents in a sorption-enhanced glycerol steam reforming process, showing H_2 production up to 85% and CO_2 removal on multi-cycle processes. This outcome was achieved due to the Ni species evolved to form stable Ni species, avoiding coke formation during the reforming reaction. Finally, Mendoza-Nieto et al. [34] proposed a modified process for H_2 production by two consecutive steps in the presence of Na_2ZrO_3 : CO_2 capture over alkaline ceramics, followed by a catalytic reaction using CO_2 captured previously as a reagent in methane dry reforming (MDR). NiO-containing Na_2ZrO_3 samples were able both trap CO_2 chemically in a wide temperature range (200–900 °C) and produce hydrogen from 500 to 900 °C, depending on the NiO load used. The H_2 production and temperature reaction were importantly improved as a function of NiO content. Thus, 10% of H_2 at 900 °C was the highest amount observed with pristine Na_2ZrO_3 ; meanwhile, H_2 production of 27% was obtained using the sample with the highest NiO content (10%wt.). Additionally, that work showed the possibility of cycling the entire process using a re-oxidized sample, positioning NiO-doped sodium zirconate as a potential bifunctional material with good performance during H_2 production through a modified MDR process. This process was proposed considering that methane dry reforming is typically performed at temperatures between 700 and 900 °C, as this reaction is an endothermic process. Ni-based catalysts are the most common materials used for DRM, considering their low cost in comparison with noble metal catalysts, including Ru-, Rh- and Pt-based catalysts. Nevertheless, problems with carbon deposition may damage Ni catalyst performance [38].

Based on all previous reports described above, the aim of the present work was to analyze the possibility of using free-nickel alkaline ceramics, such as Li_2ZrO_3 and Na_2ZrO_3 , as bifunctional materials in the following modified process: CO_2 capture continued by a subsequent MDR process. Thus, the influence of two variables (ceramic type and gas mixture used in CO_2 capture) over H_2 production was analyzed. For this purpose, different gas mixtures were employed (CO_2 , CO or $\text{CO}-\text{O}_2$).

2. Experimental section

2.1. Synthesis and characterization of alkaline zirconates

Li_2ZrO_3 and Na_2ZrO_3 were synthesized by the well-known procedure of solid-state reaction as previously reported [14,26,30]. Zirconium oxide (ZrO_2 , Aldrich) and lithium carbonate (Li_2CO_3 , Aldrich) or sodium carbonate (Na_2CO_3 , Aldrich) were used as reagents without any further treatment. Precursor salts were mechanically mixed and calcined in an air atmosphere at 900 °C for 12 h with a heating rate of 5 °C/min. Due to the high tendency of lithium and sodium to sublime at temperatures higher than 700 °C, 10 wt% of carbonate excesses were considered [39,40].

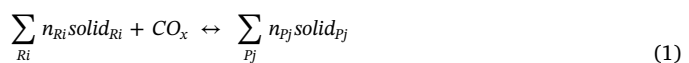
Alkaline zirconates were structural and microstructurally

characterized by powder X-ray diffraction (XRD) and N_2 adsorption-desorption. XRD patterns were recorded in the $10^\circ \leq 2\Theta \leq 80^\circ$ range with a goniometer speed of $2^\circ(2\Theta) \text{ min}^{-1}$ using a Siemens D5000 diffractometer coupled to a cobalt anode ($\lambda = 1.789 \text{ \AA}$) X-ray tube. Then, nitrogen adsorption-desorption isotherms were measured with Bel-Japan Minisor II equipment at 77 K using a multipoint technique. Prior to physisorption experiments, samples were degassed at room temperature for 12 h in vacuum ($p < 10^{-1} \text{ Pa}$). The specific surface area (S_{BET}) of each material was calculated according to the BET model.

2.2. CO_2 capture and CH_4 reforming process

CO_2 sorption ability was evaluated by performing different thermogravimetric analyses (TGA) with a TA Instruments Q500HR thermobalance. Both zirconates, Li_2ZrO_3 and Na_2ZrO_3 , were heat-treated from room temperature up to 900 °C with a heating rate of 3 °C/min. These experiments were performed with ~50 mg of sample and a total flow rate of 60 mL/min under the following gas mixtures using nitrogen (N_2 , Praxair grade 4.8) as balance gas: i) saturated CO_2 ($P_{\text{CO}_2} = 1.0$, Praxair grade 3.0), ii) diluted CO_2 ($P_{\text{CO}_2} = 0.05$), iii) diluted CO ($P_{\text{CO}} = 0.05$, Praxair certificate standard) and iv) $\text{CO}-\text{O}_2$ mixture ($P_{\text{CO}} = P_{\text{O}_2} = 0.05$, Praxair grade 2.6 for O_2). The aim of using different gas mixtures was to evaluate if CO_2 obtained through different sources affects carbonation behavior of these ceramics. Additionally, it has to be pointed out that the CO experiments were performed considering that CO oxidation can occur with alkaline ceramics producing CO_2 that is subsequently captured [30]. Additionally, some isothermal experiments were performed at 600 °C during 3 h. In these tests, the samples were heated up to 600 °C (5 °C/min) using N_2 (40 mL/min) as the carrier gas. Once the desired temperature was achieved, the flow gas was switched to a saturated CO_2 or $\text{CO}-\text{O}_2$ mixture. Afterward, isothermal products were analyzed by CO_2 Temperature-Programmed Desorption (CO_2 -TPD) with a chemisorption analyzer (Belcat, Bel-Japan) to obtain information about the desorption abilities of each material. CO_2 -TPD analyses were performed by heating each sample up to 850 °C (heating rate of 2 °C/min) in a He flow of 30 mL/min. The data were quantified by a thermal conductivity detector (TCD).

To understand and complement the experimental results obtained during the capture process, *ab initio* thermodynamic calculations were performed by combining density functional theory (DFT) with the lattice phonon dynamics approach [41]. For this purpose, capture reactions of both solids were normalized by one mol of carbon monoxide or carbon dioxide (CO_x) and expressed as follows in Eq. (1):



where n_{R_i} and n_{P_j} represent the moles of reactants (R_i) and products (P_j), respectively, involved in each reaction. The gas phase was treated as an ideal gas. By assuming that difference between chemical potentials ($\Delta\mu^0$) of reactants (R_i) and products (P_j), the value can be approximated by the difference in their total energies (ΔE^{DFT}), obtained in DFT calculations; by their vibrational free energies of phonon dynamics; and by ignoring the PV contribution terms for solids. Thus, the variation in the Gibbs free energy (ΔG) as a function of temperature and CO_x pressure can be written as follows (Eq. (2)):

$$\Delta G(T, P) = \Delta\mu^0(T) - RT \ln\left(\frac{P_{\text{CO}_x}}{P_0}\right) \quad (2)$$

where

$$\Delta\mu^0(T) \approx \Delta E^{\text{DFT}} + \Delta E_{\text{ZP}} + \Delta F^{\text{PH}}(T) - G_{\text{CO}_x}^0(T) \quad (3)$$

Here, ΔE^{DFT} is the DFT energy difference between the reactants and products. ΔE_{ZP} is the zero point energy difference between the reactants and products obtained directly from phonon calculations. ΔF^{PH} is the phonon free energy change excluding zero-point energy (which is

already counted into ΔE_{ZP} term) between the product and reactant solids. P_{CO_x} is the partial pressure of the corresponding carbon oxide in the gas phase, and P_0 is the standard state reference pressure equal to 1 bar. The heat of reaction [$\Delta H^{cal}(T)$] was evaluated through the Eq. (4):

$$\Delta H^{cal}(T) = \Delta\mu^0(T) + T[\Delta S_{PH} - S_{CO_x}(T)] \quad (4)$$

where $\Delta S_{PH}(T)$ is the difference in entropies between the product and reactant solids. The free energy of CO_x ($G^{\circ}_{CO_x}$) can be obtained from standard statistical mechanics, and its entropy (S_{CO_x}) can be found in empirical thermodynamic databases. [42].

Afterward, the lithium and sodium zirconates were tested in the methane dry reforming (MDR) reaction following the procedure reported in previous works [34,36]. The samples (200 mg) were introduced in a Bel-Rea catalytic reactor from Bel-Japan and carbonated dynamically from 30 to 600 °C (heating rate of 5 °C/min). They were then isothermally treated at 600 °C for 1.0 h under four gas mixtures described above in TGA analysis using a total flow of 100 mL/min. Then, the samples were cooled to 400 °C using the same gas mixture. Once each sample was carbonated, the MDR process was performed from 400 to 900 °C with a heating rate of 2 °C/min using 100 mL/min of a gas mixture composed of CH_4 (5 vol%, Praxair grade 5.0) and N_2 . Moreover, cyclic experiments of CO_2 capture and subsequent MDR tests were performed with both zirconates at the best carbonation condition ($CO-O_2$ gas mixture). This double procedure was performed repeating the same experimental conditions described above during six cycles. In all cases, the concentration of reforming gas products was obtained every 15 °C until 900 °C (dynamic experiments), using a Shimadzu GC-2014 gas chromatograph with a Carbonex-1000 column. The hydrogen production efficiency was calculated as follows:

$$\% H_2 = \frac{[H_2]_i}{2 [CH_4]_0} \times 100 \quad (5)$$

where $[H_2]_i$ is the hydrogen concentration at each temperature, and $[CH_4]_0$ is the initial concentration of methane. After MDR reactions, some of these catalytic materials were re-characterized by powder X-ray diffraction and N_2 adsorption-desorption.

3. Results and discussion

3.1. Characterization of alkaline zirconates

Powder XRD patterns for both alkaline zirconates are shown in Fig. 1A. As expected, Na_2ZrO_3 (PDF 35-0770 file) and Li_2ZrO_3 (PDF 75-2157 file) crystalline planes were the main phases observed in sodium and lithium zirconates, respectively. In particular, lithium-based sample presented a different reflection located at 21.4°, in 2θ scale, which can be related to Li_4ZrO_4 (PDF 20-0645 file). The presence of this secondary phase with a higher Li atom concentration can be explained by the excess Li used during the synthesis stage. Then, N_2 adsorption-desorption was used to determine the textural characteristics of alkaline zirconates. Nitrogen adsorption-desorption isotherms are shown in Fig. 1B. According to IUPAC classification, both materials present type II isotherms related to nonporous materials [43] with no significant hysteresis loops. Additionally, specific surface areas (S_{BET}) were determined from N_2 adsorption curves using the BET model. The S_{BET} of the sodium sample ($3.0 \text{ m}^2/\text{g}$) was three times higher than that of lithium zirconate ($1.0 \text{ m}^2/\text{g}$). These values are in line with the synthesis method used. Additionally, N_2 adsorption-desorption results are in good agreement with previous reports for alkaline zirconates synthesized by the solid-state reaction [12,30,44].

3.2. Effect of carbonation condition on capture and catalytic performances

3.2.1. Lithium zirconate (Li_2ZrO_3)

After the characterization stage, lithium zirconate was thermally treated from 30 to 950 °C into a thermobalance with the aim of determining its CO_2 capture abilities under different gas mixtures described in the experimental section. Thermograms are presented in Fig. 2A, showing a bimodal distribution as a function of temperature. According to the literature [13], the first weight increment (low temperature) is related with a superficial capture, whereas the second weight increment (high temperature) corresponds to volumetric CO_2 capture promoted by diffusion processes into the ceramic, allowing bulk CO_2 chemisorption. Regarding the first process, between 150 and 400 °C, Li_2ZrO_3 only demonstrated a weight increment of 0.4 wt% using a $P_{CO_2} = 1.0$. In this step, a thin $Li_2CO_3-ZrO_2$ external shell was formed over Li_2ZrO_3 particles (R1). When all other gases were used, CO_2 superficial chemisorption was almost negligible. In fact, these profiles

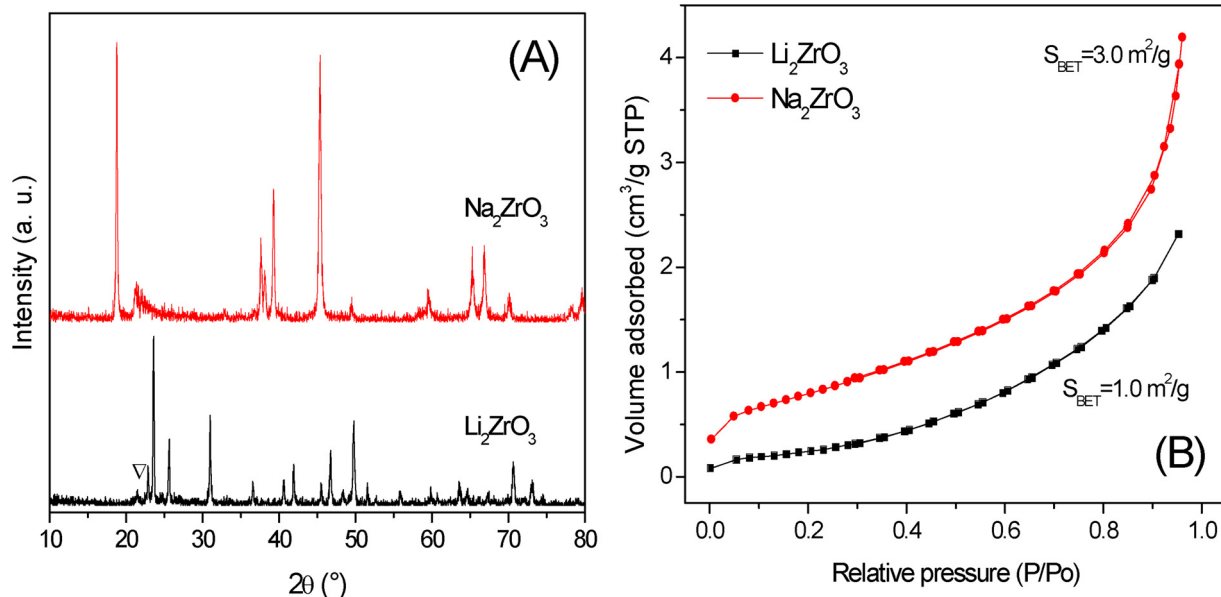


Fig. 1. XRD patterns (A) and N_2 adsorption-desorption isotherms (B) for Li_2ZrO_3 and Na_2ZrO_3 materials. (∇) Li_4ZrO_4 crystalline phase.

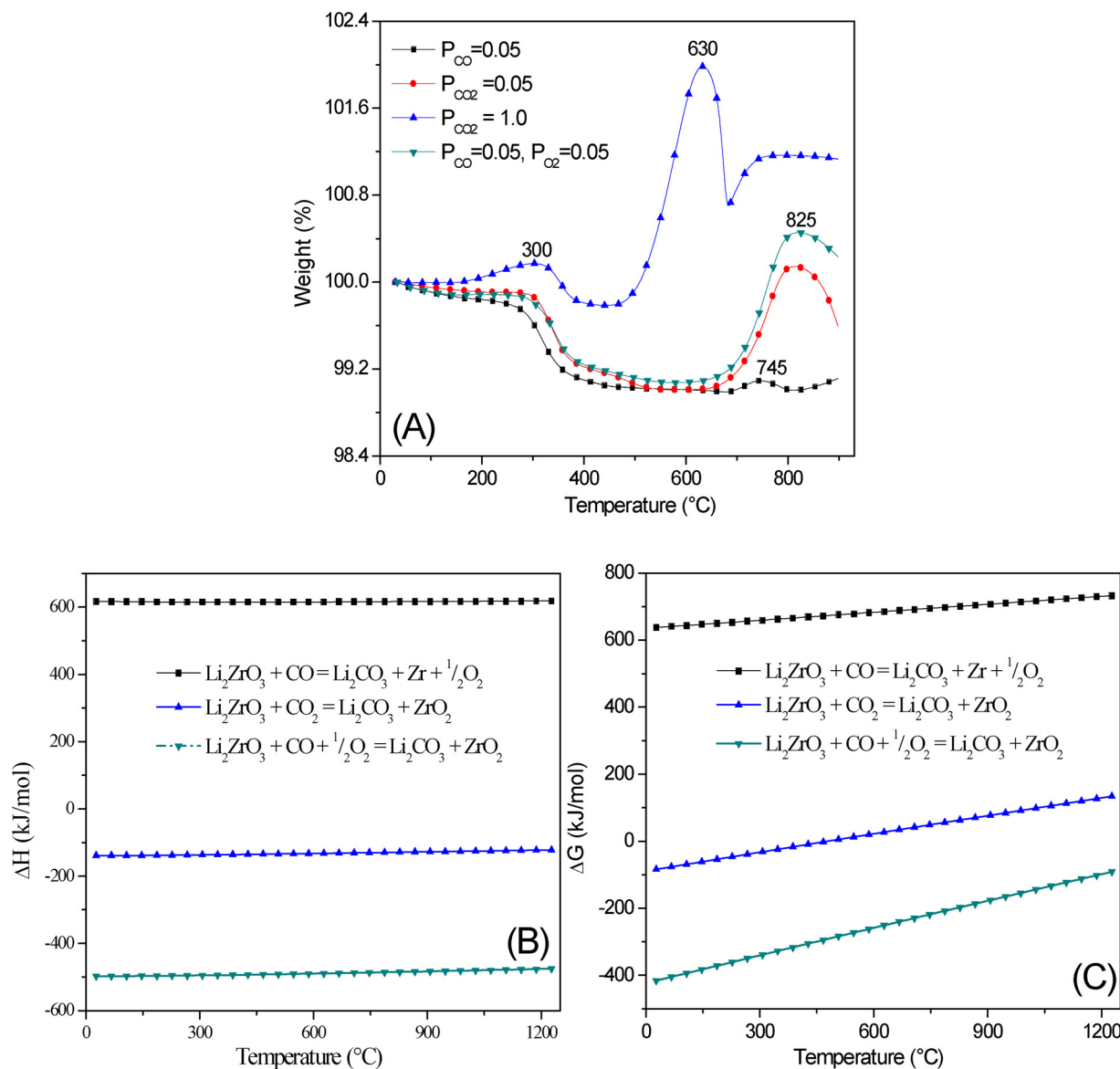
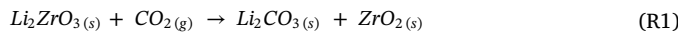


Fig. 2. Thermogravimetric analysis of Li_2ZrO_3 tested dynamically under different gas mixtures (A), theoretical enthalpy (B) and Gibbs free energy (C) for each corresponding reaction.

presented a weight decrease, which may be related to sample dehydroxylation.



In contrast, the volumetric process was presented independently of the gas used, although bulk chemisorption strongly depended on the gas mixture. It has been reported that Li-containing ceramics are able to chemisorb CO or CO_2 at high temperatures, e.g., Li_2CuO_2 [45,46] captures CO_2 directly, whereas in the CO case, carbon monoxide oxidation occurs first, followed by the CO_2 capture process. In line with this outcome, lithium zirconate was also able to chemisorb both carbon oxides with some interesting differences. When CO was used, the smallest capture was observed at approximately 745 °C, followed by diluted CO_2 and $\text{CO}-\text{O}_2$ cases, which presented similar weight increments (1.1–1.4 wt%) at higher temperatures (~825 °C). On the other hand, saturated CO_2 gas flow was the condition with the highest CO_2 capture (2.0 wt% at 630 °C) in the lowest temperature range (470–700 °C). In the last case, CO_2 volumetric capture was at least ten times higher than the superficial process discussed above. Moreover, the dynamic thermograms show that using low CO_2 or $\text{CO}-\text{O}_2$ partial

pressures importantly modified the CO_2 chemisorption equilibrium on Li_2ZrO_3 .

To corroborate these experimental observations, some theoretical calculations were performed. Fig. 2B and C show molar enthalpy (ΔH) and Gibbs free energy (ΔG) profiles as a function of temperature for three main reactions tested in the carbonation process. CO oxidation in the absence of O_2 is an endothermic and non-spontaneous reaction in all temperature ranges and fits well with the experimental data. The lowest capture was obtained due to CO must react with oxygen atoms located in the crystalline network of ceramic and then produce CO_2 that can be chemisorbed in a subsequent step. In contrast, lithium zirconate carbonated with a $\text{CO}-\text{O}_2$ gas mixture presented an exothermic and spontaneous behavior, showing that CO_2 production is benefited under this condition. Regarding direct CO_2 capture, this reaction is also an exothermic reaction. Nevertheless, it is only spontaneous at $T < 500$ °C; meanwhile, at higher temperatures, this reaction switches to non-spontaneous behavior. As can be seen, Li_2ZrO_3 is able to chemisorb CO or CO_2 at different temperatures as a function of temperature and gas used. However, the $\text{Li}_2\text{CuO}_2-\text{CO}-\text{O}_2$ system presented the best thermodynamic results for a carbonation process. This result is

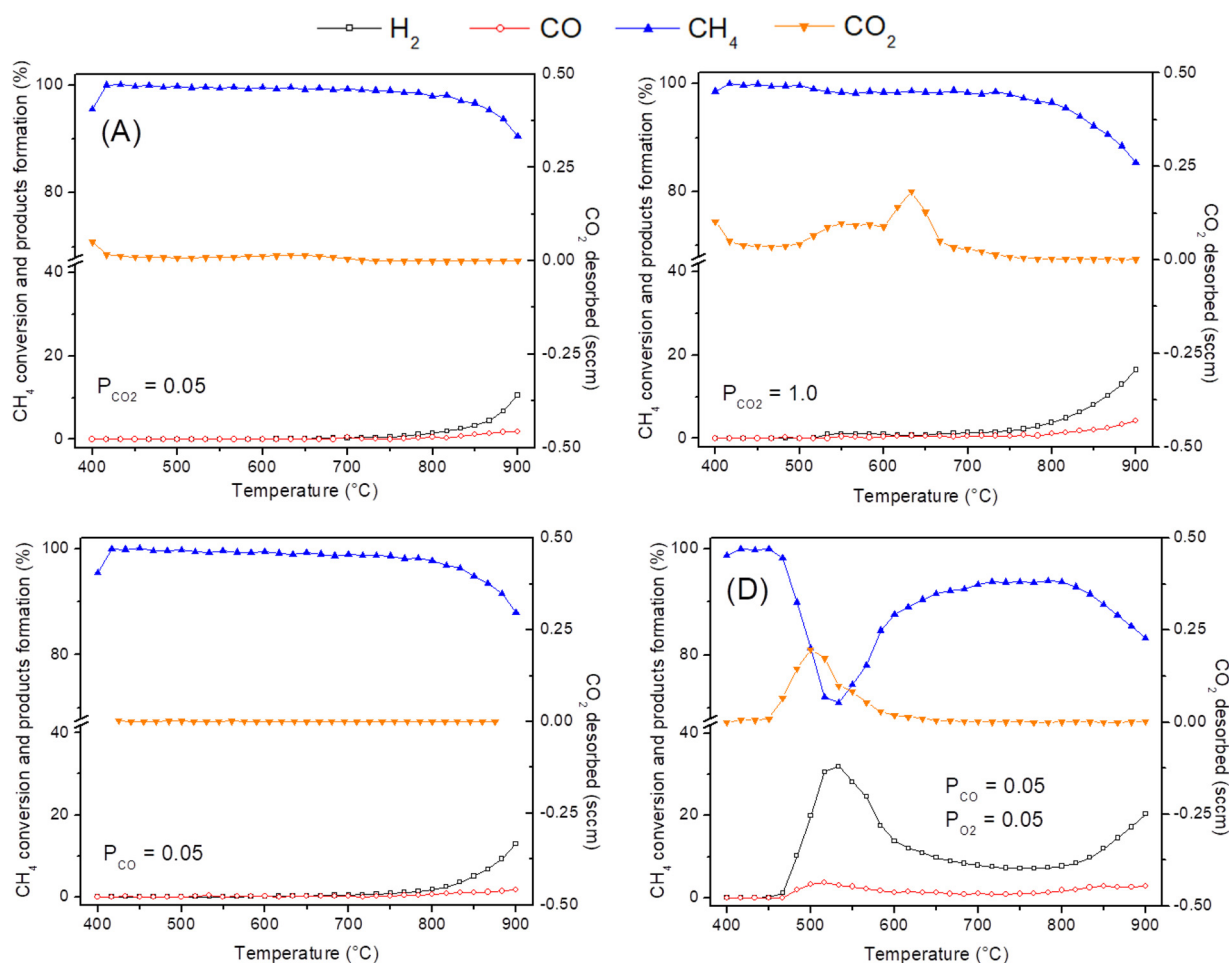
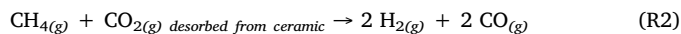


Fig. 3. Dynamic evolution of reactants (CO_2 and CH_4) and products (CO and H_2) obtained after consecutive CO_2 capture and CH_4 dry reforming, using Li_2ZrO_3 with different gas mixtures during the carbonation process. CO_2 quantification is not possible, as it is desorbed from ceramic materials. Thus it is only reported in sccm units.

interesting, as it has been reported [34,36,47] that carbonated-ceramics can be used as a CO_2 source for H_2 production through a catalytic process: methane dry reforming (MDR, R2). Thus, lithium zirconate presented attractive capture properties for being used in these consecutive processes: CO_2 capture-MDR.



After dynamic CO_2 capture analysis, a two-step process was proposed with the aim to produce syngas, ($\text{H}_2 + \text{CO}$). This process consisted of CO_2 capture on Li_2ZrO_3 ceramic followed by a catalytic stage between methane (CH_4) and the previously captured CO_2 . In line with previously published methods [34,47], the carbonation process was performed at 600 °C under the four gas mixtures tested in TGA analyses, although some gas compositions did not present the best CO_2 chemisorption on Li_2ZrO_3 at this temperature (Fig. 2A). Reactants (CH_4 and CO_2) and products that evolved (H_2 and CO) are shown in Fig. 3 as a function of temperature. When Li_2ZrO_3 was carbonated with CO or CO_2 (diluted and saturated), H_2 production was detected only at high temperatures ($T > 700$ °C), indicating that this process occurs mainly through a partial methane oxidation (POM), because CO_2 desorption was not observed between 700–900 °C but at lower temperatures (~550–680 °C). In these three cases, H_2 formation fits well with CH_4 reduction content (Fig. 3, A–C charts), reaching efficiencies between 11 and 16% at 900 °C with H_2/CO ratios greater than 1.0. According to the literature [48], the reverse water-gas shift (RWGS) reaction can occur. However, the formed H_2 cannot react with CO_2 due to the desorption process from carbonated- Li_2ZrO_3 , as it was not observed at $T > 700$ °C.

In contrast, catalytic evolution for the Li_2ZrO_3 sample carbonated under $\text{CO}-\text{O}_2$ condition showed a different behavior for the MDR reaction (Fig. 3D). In this case, hydrogen production shows two maxima at 550 and 900 °C with 31.9 and 20.6% efficiencies, respectively. These results must be related to theoretical calculations presented in Fig. 2B, where the $\text{CO}-\text{O}_2$ gas mixture was the most stable reaction for obtaining a carbonated ceramic. Then, in the low-temperature range, H_2 and CO productions were observed; meanwhile, CH_4 decreased and CO_2 was desorbed from the ceramic, confirming that the MDR reaction occurred. The H_2/CO ratio was higher than 1.0 between 450 and 650 °C, being in the maximum point equal to 10, suggesting a feasible RWGS reaction; however, H_2O was not detected as a product in this experiment. Regarding catalytic behavior at $T > 800$ °C, syngas production was obtained without CO_2 desorption, suggesting that partial CH_4 oxidation had taken place, similar to those cases previously described. Additionally, H_2/CO ratios were higher than 1.0 at high temperatures, showing the selectivity of these carbonated materials. These results clearly showed that Li_2ZrO_3 can act not only as a CO_2 sorbent but also as a catalyst with a high selective preference to H_2 formation, positioning it as a promising material for producing a clean energy source under moderate temperatures.

3.2.2. Sodium zirconate (Na_2ZrO_3)

Sodium zirconate was evaluated as bifunctional material (sorbent-catalyst) for the double process proposed in a similar way as described above. TGA analyses (Fig. 4A) were performed under the four gas mixtures described in the experimental section. Sodium zirconate

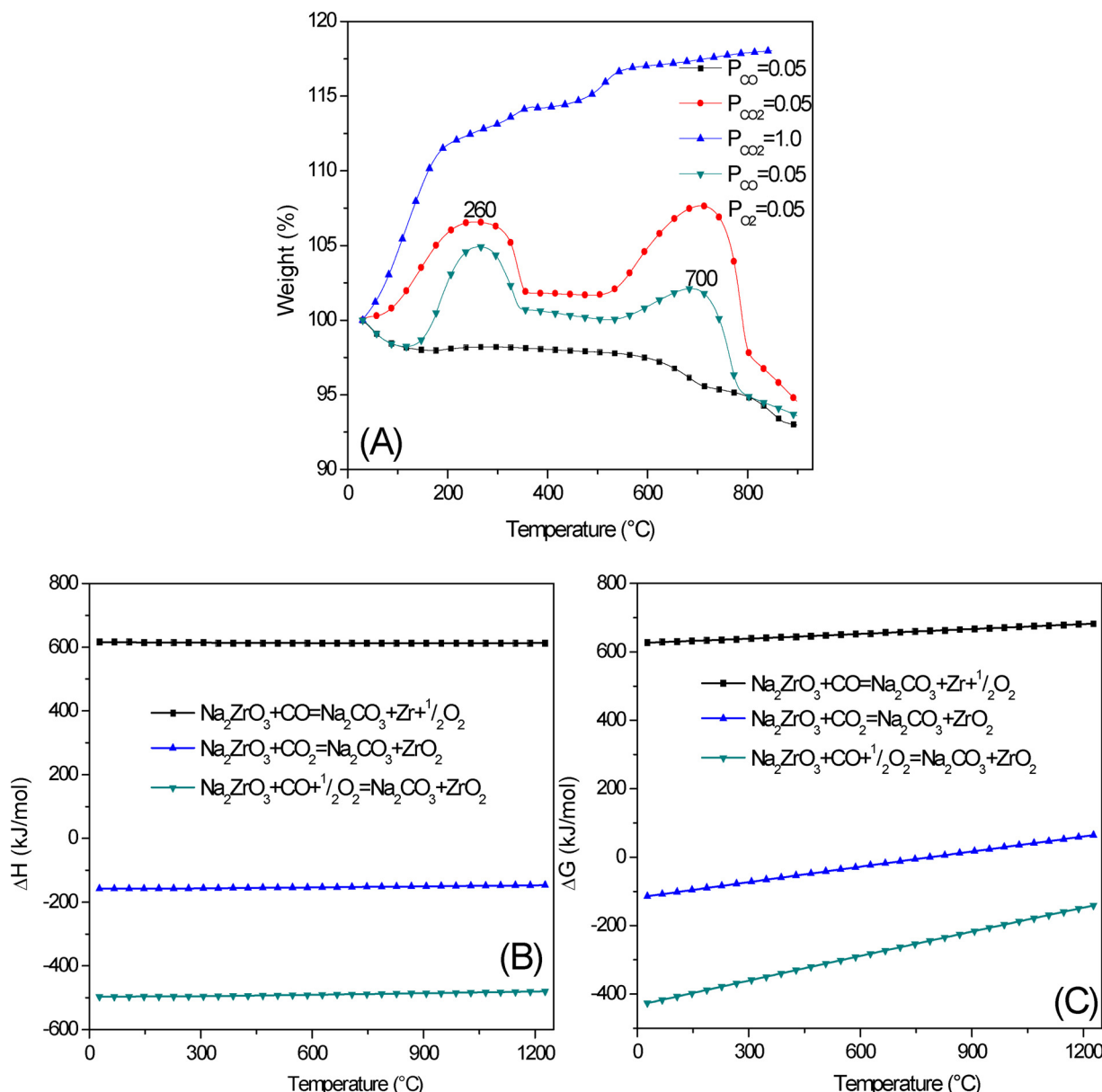


Fig. 4. Thermogravimetric analysis of Na_2ZrO_3 tested dynamically under different gas mixtures (A), theoretical enthalpy (B) and Gibbs free energy (C) for each corresponding reaction.

showed higher CO_2 captures than those of Li_2ZrO_3 (see Fig. 2A). Then, it could be observed that the weight increments in thermal profiles showed the following trend as a function of gas mixture used: saturated $CO_2 >$ diluted $CO_2 > CO-O_2 > CO$. A poor capture was observed with CO . In contrast, a saturated CO_2 profile presented a continuous increasing trend, obtaining the highest chemisorption (18.0 wt%) at 900 °C. Finally, diluted CO_2 and $CO-O_2$ profiles presented intermediate captures in a bimodal behavior with maxima at 260 and 700 °C, related with superficial and volumetric processes, respectively. These two cases presented CO_2 desorption at approximately 320 °C due to superficial CO_2 chemisorption-desorption equilibrium modifications produced by the low CO or CO_2 partial pressures.

With the aim of obtaining further information, enthalpy (ΔH) and Gibbs free energy (ΔG) were calculated for the different gas flows tested (Fig. 4B and C). Na_2ZrO_3 showed the same trend as Li_2ZrO_3 : 1) ceramic carbonation with CO is an endothermic and non-spontaneous process, 2) the $Na_2ZrO_3-CO-O_2$ reaction is an exothermic and spontaneous reaction, and 3) CO_2 direct carbonation is an exothermic reaction between 30–1200 °C with a switch from spontaneous to non-spontaneous

at 780 °C. Similar to the lithium case, Na_2ZrO_3 is able to chemisorb CO or CO_2 and trap it, showing the best condition under $CO-O_2$ gas flow. This result is in good agreement with previous reports [12,30].

Considering TGA and theoretical results, only saturated CO_2 and $CO-O_2$ conditions were used for accomplishing the double process of CO_2 capture- CH_4 dry reforming with sodium zirconate. The catalytic results are shown in Fig. 5. In both cases, the MDR reaction was the first process performed through the CO_2 desorption from ceramic and subsequent chemical reaction with methane; then, the POM reaction took place at $T > 750$ °C without CO_2 desorption. Regarding CO_2 conditions (Fig. 5A) between 650 and 750 °C, the MDR reaction took place, reaching hydrogen formations up to 5.2% with H_2/CO ratios close to 1.0; meanwhile, between 650–900 °C, the second process was observed, obtaining the highest H_2 production at 900 °C (21.4%) with a high selectivity ratio ($H_2/CO = 8.2$) at 900 °C. In contrast, when the $CO-O_2$ mixture (Fig. 5B) was used, the MDR reaction switched to lower temperatures (400–650 °C); meanwhile, the POM reaction occurred at the same temperature range. Unlike the CO_2 condition, the $CO-O_2$ gas mixture promoted outstanding H_2/CO ratios at 540 °C ($H_2/CO = 15.0$)

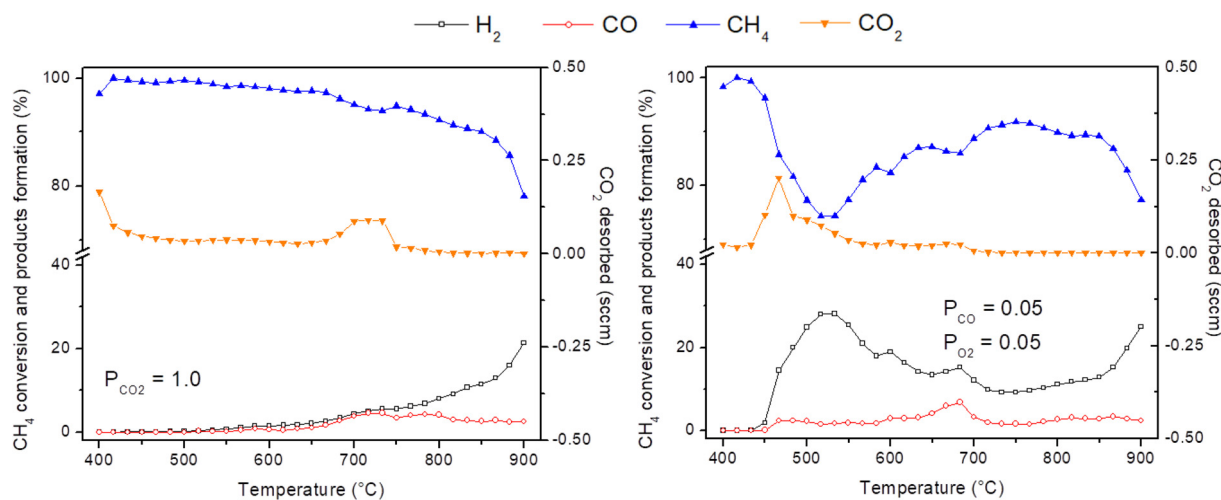


Fig. 5. Dynamic evolution of reactants (CO_2 and CH_4) and products (CO and H_2) obtained after CO_2 capture and CH_4 dry reforming using Na_2ZrO_3 with different gas mixtures during the carbonation process. CO_2 average quantification is not possible, as it is desorbed from ceramic materials. Thus it is only reported in sccm units.

and 900 °C ($H_2/CO = 11.2$), pointing out high Na_2ZrO_3 selectivity during the catalytic process. Despite the high H_2/CO ratio obtained with sodium ceramic, RWGS reaction did not occur because H_2O was not observed among the products detected by chromatography.

3.3. Effects of alkali metal over capture, desorption and catalytic characteristics

To further understand the double process produced on both zirconates, a comparison of capture, desorption and catalytic properties on both alkaline zirconates, was performed. First, some isothermal experiments were performed at 600 °C over 3 h to determine the main differences during the carbonation step that, according to results described above, is a key step for the subsequent catalytic process. Thermal profiles for CO_2 capture are shown in Fig. 6A. In general, the sodium ceramic presented higher weight increments than the lithium ceramics regardless of the gas mixture used, reaching 19.7 wt% under CO_2 and 9.7 wt% with the $CO-O_2$ gas mixture. CO_2 capture was higher when using CO_2 than $CO-O_2$. This result is quite interesting considering that catalytic tests described above showed that CO_2 gas flow did not allow obtaining high hydrogen productions. Then, desorption tests

were carried out with products obtained from these isothermal experiments. CO_2 -desorption profiles (Fig. 6B) for sodium samples presented well-defined distributions, contrary to the lithium profiles. This result is related with the amount of CO_2 captured in TGA analyses. The Na_2ZrO_3 sample under CO_2 gas flow presented a desorption signal between 600–800 °C with a maximum at 715 °C, showing the highest gas-solid interaction among all samples tested. When $CO-O_2$ was used, a weaker interaction between the captured CO_2 and Na_2ZrO_3 was observed, showing a maximum CO_2 desorption at 680 °C. Similar results were obtained on lithium sample profiles as described in the previous section. In the $CO-O_2$ case, the CO_2 desorption began earlier than that in the CO_2 case. However, as is shown in Fig. 6B, Li_2ZrO_3 did not show a specific temperature in which most of the CO_2 was desorbed, CO_2 desorption was produced during a wide temperature range. Moreover, it must be pointed out that despite the fact that higher amounts of CO_2 were captured under the CO_2 condition for both ceramics, CO_2 presented a high interaction with solids and then a higher desorption temperature, which is not beneficial for the subsequent catalytic reaction (MDR). Thus, in the $CO-O_2$ gas mixture, it is possible to capture CO_2 , but the interaction between gas and the ceramic is weak, allowing it to desorb it easily during the MDR process.

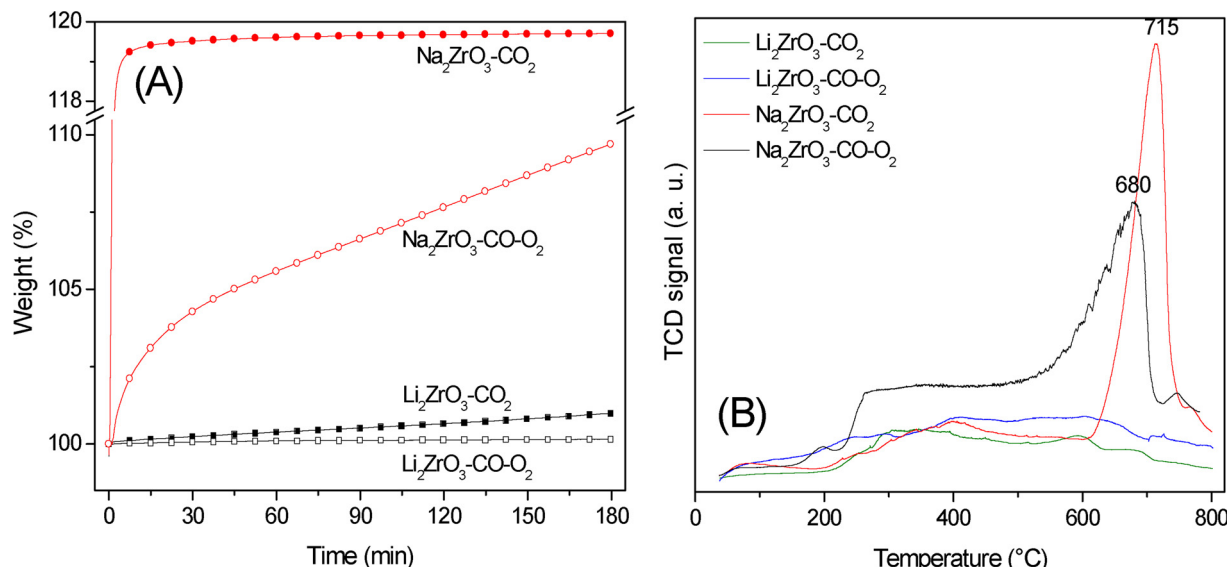


Fig. 6. Isothermal profiles obtained at 600 °C during 3 h of carbonation (A) and CO_2 -TPD analyses (B) for Li_2ZrO_3 and Na_2ZrO_3 carbonated under saturated CO_2 and $CO-O_2$ gas flows, using a thermal conductivity detector.

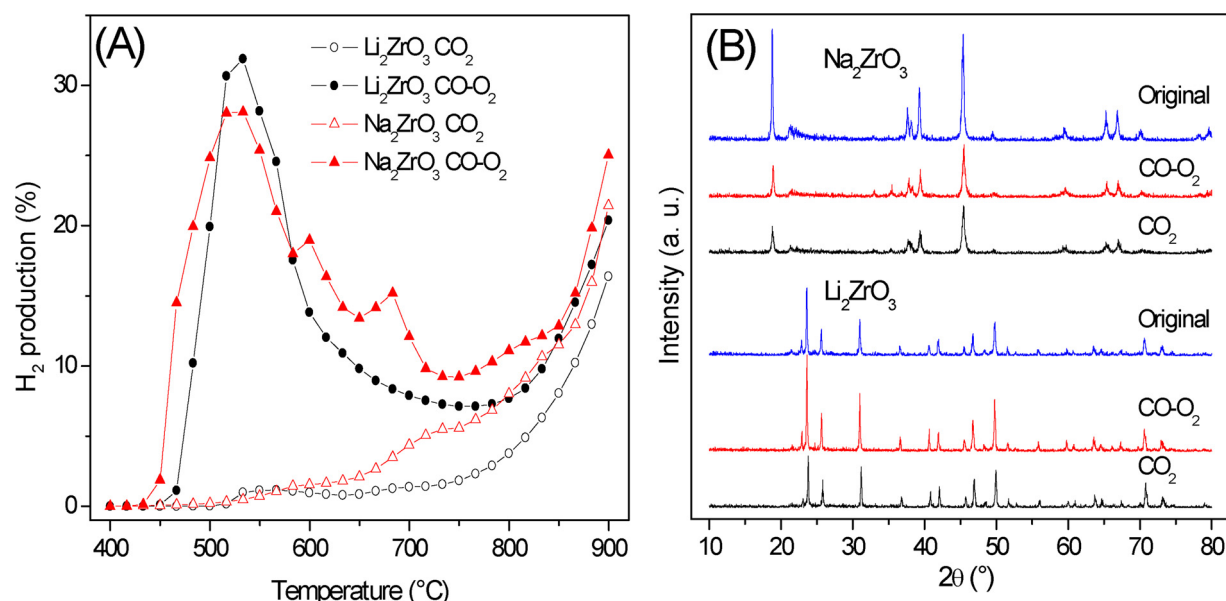


Fig. 7. H₂ production for Li₂ZrO₃ and Na₂ZrO₃ carbonated samples with saturated CO₂ or CO-O₂ gas mixtures (A) and XRD patterns of products obtained after the double carbonation-MDR process (B).

Fig. 7A shows a comparison of hydrogen formation (catalytic results) as a function of the condition of carbonation used. In general, similar thermal profiles can be obtained when both ceramics were tested under the same carbonation condition. When the CO-O₂ gas mixture was used, hydrogen productions and reaction temperatures were highly improved in comparison with saturated CO₂. In the CO-O₂ case, both ceramics presented good H₂ production, approximately 28–32%, at moderate temperatures (450–600 °C), which is in good agreement with CO₂ desorption temperatures from alkaline ceramics, promoting MDR. At higher temperatures, H₂ production tended to decrease between 600 and 760 °C, as most of the CO₂ must have been already desorbed. Finally, at temperatures higher than 780 °C, H₂ production increased again, but in this case, it was produced by the POM process. It must be pointed out that the Li₂ZrO₃ sample produced similar H₂ amounts as Na₂ZrO₃, although Li₂ZrO₃ trapped smaller amounts of CO₂ (see Fig. 6). Thus, Li₂ZrO₃ presented a more efficient MDR reaction than Na₂ZrO₃. This effect may be produced by the differences observed in TPD results, where CO₂ desorption was slower on Li₂ZrO₃ than that on Na₂ZrO₃, enabling a higher interaction and reactivity between CO₂ and CH₄ on Li₂ZrO₃. In contrast, when carbonation was produced with CO₂, none of these samples produced H₂ between 450 and 650 °C and only POM was produced at higher temperatures.

Both zirconates seem to be good bifunctional materials (sorbent-catalyst) with high abilities in the double process proposed; the carbonation that was followed by MDR had the best results using a CO-O₂ gas mixture as a carbonation source. Then, the regeneration abilities after the double process were studied in both ceramics through DRX analyses (Fig. 7B). In all products, a good regeneration was achieved, regardless of the gas condition or ceramic used. X-Ray diffraction patterns showed a primary crystalline phase for lithium or sodium zirconate without the presences of secondary phases.

Finally, cyclability for the double process was evaluated using the best carbonation gas flow (CO-O₂). Thermal profiles of six cycles are shown in Fig. 8 for both ceramics. Hydrogen production did not decrease significantly in both cases, showing that carbonated-ceramics can be used several times as catalytic materials for the MDR reaction. All profiles obtained showed the same bimodal distributions described in the previous sections: i) MDR at T < 750 °C and ii) partial CH₄ oxidation at T > 750 °C. However, there are some differences as a function of alkaline zirconate. Despite the fact that lithium zirconate

was able to capture small amounts of CO₂, it presented high desorption abilities, maintaining H₂ formation through the cycles. The first distribution presented a maximum at 565 °C for cycle one (37.7%) whereas in the rest of the cycles, the temperature was shifted to 520 °C with H₂ production maxima between 33.1 and 35.5%. In contrast, hydrogen production was obtained at high temperatures by POM with changes as a function of cycles. It increased from 28.3 to 44.8% between cycles one and six. This outcome means that the partial oxidation process was enhanced by 58.1% after six consecutive carbonation-MDR cycles. A different catalytic behavior was obtained with sodium zirconate. In this case, both distributions were enhanced through cycles. Initial H₂ production (MDR process) increased from 18 to 35%, while H₂ production derived from POM increased from 20 to 25% for both reaction processes between the first and sixth cycles.

To understand this phenomenon, alkaline ceramic products obtained after the sixth cycle were re-characterized by the N₂ adsorption-desorption technique (Fig. 9). These isotherms presented the same characteristics as pristine materials (isotherms type II with no hysteresis loop), although both products showed isotherms with larger amounts of N₂ adsorbed, resulting in specific surface areas almost twice larger than pristine ceramics. Surface area increments, on both samples, may be attributed to partial particle fracture produced during carbonation-decarbonation cycles, as carbonates have different densities than alkaline zirconates. Based on DRX, catalytic and N₂ adsorption-desorption results shown in this section, it can be established that not only ceramic regeneration was possible to achieve after catalytic tests, but deactivation processes were also not observed after several cycles, indicating the high thermal stability of both alkaline ceramics.

4. Conclusions

According to the capture, desorption and catalytic results, the following statements can be established:

- Both alkaline zirconates were able to chemisorb CO and CO₂ in wide temperature ranges (200–900 °C), showing that direct CO₂ carbonation is favored over CO₂ carbonation produced from previous CO oxidation processes.
- Regardless of the type of alkaline zirconate used, CO oxidation was carried out when oxygen was added in the gas flow, followed by a subsequent CO₂ chemisorption.

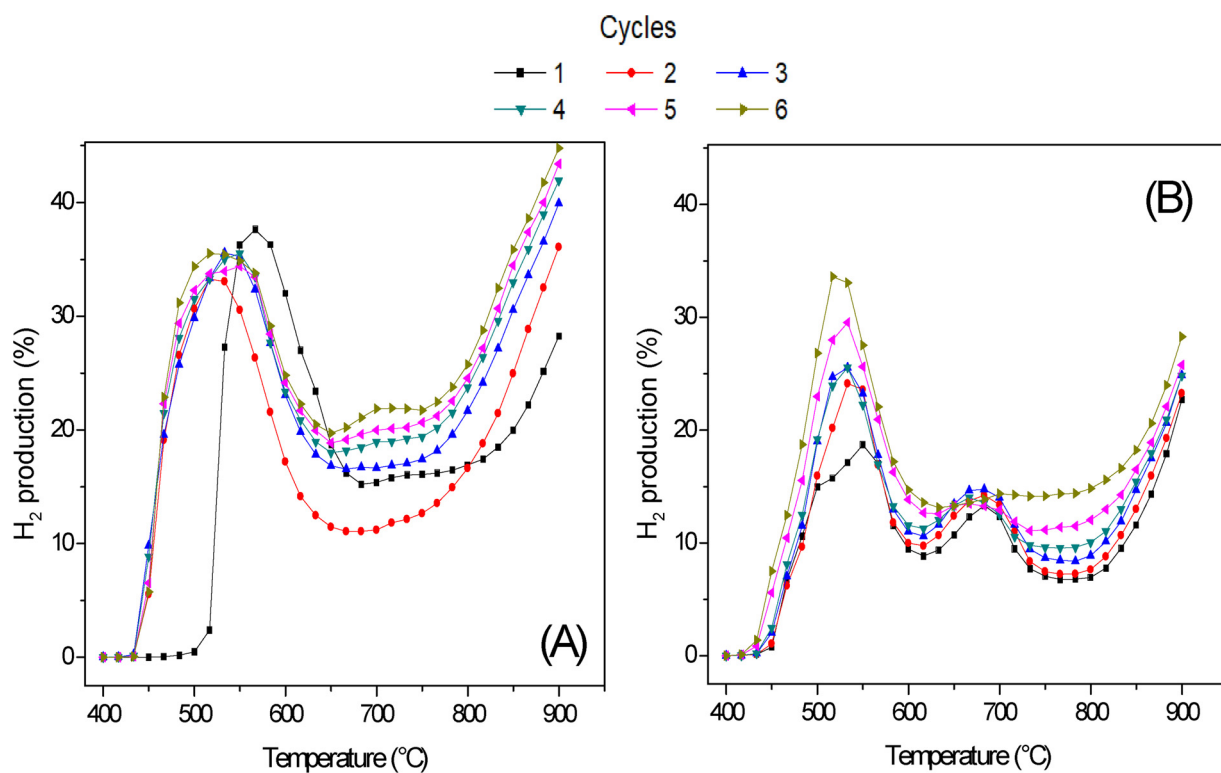


Fig. 8. Cyclic tests of carbonation-MDR processes for Li_2ZrO_3 (A) and Na_2ZrO_3 (B).

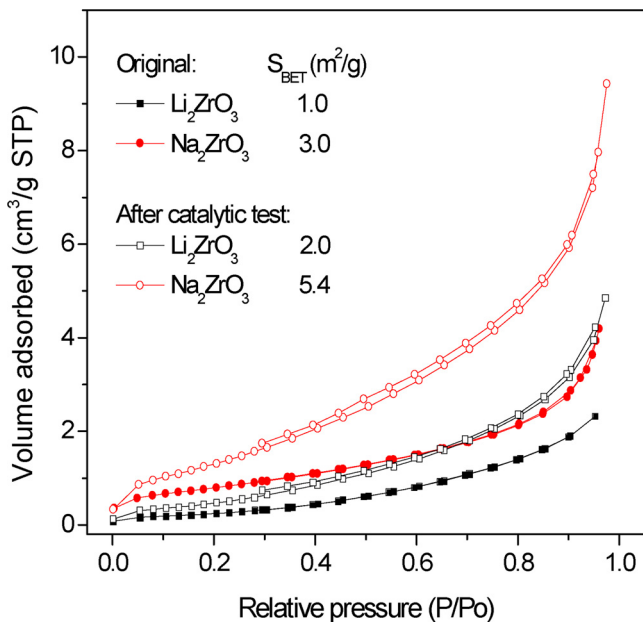


Fig. 9. N_2 adsorption-desorption isotherms of Li_2ZrO_3 and Na_2ZrO_3 initial samples and products obtained after carbonation-MDR cycles.

- Despite the fact that CO_2 captures were higher under saturated CO_2 in comparison with the $\text{CO}-\text{O}_2$ case, a better CO_2 desorption behavior was obtained for the latter condition.
- Regardless of the carbonation condition used, alkaline ceramics were able to produce H_2 through the POM reaction at temperatures higher than 750 °C.
- The $\text{CO}-\text{O}_2$ condition was the best carbonation gas flow for obtaining carbonated ceramics with high catalytic activity in the MDR reaction in a moderate temperature range (450–700 °C).
- Lithium and sodium ceramics carbonated under the $\text{CO}-\text{O}_2$ gas

mixture also presented high regeneration and cyclability in the double process proposed: CO_2 capture-MDR reaction.

Acknowledgments

This work was financially supported by projects SENER-CONACYT (251801) and PAPIIT-UNAM (IN-101916). The authors thank A. Tejeda for technical help.

References

- K. Nakagawa, T. Ohashi, A novel method of CO_2 capture from high temperature gases, *J. Electrochem. Soc.* 145 (1998) 1344–1346, <https://doi.org/10.1149/1.1838462>.
- M.T. Dunstan, A. Jain, W. Liu, S.P. Ong, T. Liu, J. Lee, K.A. Persson, S.A. Scott, J.S. Dennis, C.P. Grey, Large scale computational screening and experimental discovery of novel materials for high temperature CO_2 capture, *Energy Environ. Sci.* 9 (2016) 1346–1360, <https://doi.org/10.1039/C5EE03253A>.
- L.K.G. Bhatta, S. Subramanyam, M.D. Chengala, S. Olivera, K. Venkatesh, Progress in hydrotalcite like compounds and metal-based oxides for CO_2 capture: a review, *J. Clean. Prod.* 103 (2015) 171–196, <https://doi.org/10.1016/j.jclepro.2014.12.059>.
- M.T. Dunstan, S.A. Mauger, W. Liu, M.G. Tucker, O.O. Taiwo, B. Gonzalez, P.K. Allan, M.W. Gaultois, P.R. Shearing, D.A. Keen, A.E. Phillips, M.T. Dove, S.A. Scott, J.S. Dennis, C.P. Grey, In situ studies of materials for high temperature CO_2 capture and storage, *Faraday Discuss.* 192 (2016) 217–240, <https://doi.org/10.1039/C6FD00047A>.
- S. Wang, S. Yan, X. Ma, J. Gong, Recent advances in capture of carbon dioxide using alkali-metal-based oxides, *Energy Environ. Sci.* 4 (2011) 3805, <https://doi.org/10.1039/c1ee01116b>.
- B. Tsuchiya, S. Nagata, T. Sugiyama, K. Tokunaga, Effects of ion irradiation on H_2O and CO_2 absorption and desorption characteristics of Li_2ZrO_3 and Pt-coated Li_2ZrO_3 , *Int. J. Hydrogen Energy* 42 (2017) 23746–23750, <https://doi.org/10.1016/j.ijhydene.2017.04.220>.
- M.T. Dunstan, H. Laeverenz Schlogelhofer, J.M. Griffin, M.S. Dyer, M.W. Gaultois, C.Y. Lau, S.A. Scott, C.P. Grey, Ion dynamics and CO_2 absorption properties of Nb-, Ta-, and Y-doped Li_2ZrO_3 studied by solid-state NMR, thermogravimetry, and first-principles calculations, *J. Phys. Chem. C* 121 (2017) 21877–21886, <https://doi.org/10.1021/acs.jpcc.7b05888>.
- L. Martínez-dlCruz, H. Pfeiffer, Toward understanding the effect of water sorption on lithium zirconate (Li_2ZrO_3) during its carbonation process at low temperatures, *J. Phys. Chem. C* 114 (2010) 9453–9458, <https://doi.org/10.1021/jp1020966>.
- M.B.I. Chowdhury, M.R. Quddus, H.I. DeLasa, CO_2 capture with a novel solid fluidizable sorbent: thermodynamics and temperature programmed

carbonation-decarbonation, Chem. Eng. J. 232 (2013) 139–148, <https://doi.org/10.1016/j.cej.2013.07.044>.

[10] T. Zhao, M. Rønning, D. Chen, Preparation of nanocrystalline Na_2ZrO_3 for high-temperature CO_2 acceptors: chemistry and mechanism, J. Energy Chem. 22 (2013) 387–393, [https://doi.org/10.1016/S2095-4956\(13\)60050-9](https://doi.org/10.1016/S2095-4956(13)60050-9).

[11] G. Ji, M.Z. Memon, H. Zhao, M. Zhao, Experimental study on CO_2 capture mechanisms using Na_2ZrO_3 sorbents synthesized by soft chemistry method, Chem. Eng. J. 313 (2017) 646–654, <https://doi.org/10.1016/j.cej.2016.12.103>.

[12] J.A. Mendoza-Nieto, H. Pfeiffer, Thermogravimetric study of sequential carbonation and decarbonation processes over Na_2ZrO_3 at low temperatures (30–80 °C): relative humidity effect, RSC Adv. 6 (2016) 66579–66588, <https://doi.org/10.1039/C6RA1253F>.

[13] L. Martínez-dlCruz, H. Pfeiffer, Cyclic CO_2 chemisorption–desorption behavior of Na_2ZrO_3 : structural, microstructural and kinetic variations produced as a function of temperature, J. Solid State Chem. 204 (2013) 298–304, <https://doi.org/10.1016/j.jssc.2013.06.014>.

[14] L. Martínez-dlCruz, H. Pfeiffer, Microstructural thermal evolution of the Na_2CO_3 phase produced during a Na_2ZrO_3 – CO_2 chemisorption process, J. Phys. Chem. C 116 (2012) 9675–9680, <https://doi.org/10.1021/jp301917a>.

[15] K.M. Ooi, S.P. Chai, A.R. Mohamed, M. Mohammadi, Effects of sodium precursors and gelling agents on CO_2 sorption performance of sodium zirconate, Asia-Pac. J. Chem. Eng. (2015) 565–579, <https://doi.org/10.1002/ajpc.1903>.

[16] H.R. Radfarnia, M.C. Iliuta, Surfactant-template/ultrasound-assisted method for the preparation of porous nanoparticle lithium zirconate, Ind. Eng. Chem. Res. 50 (2011) 9295–9305, <https://doi.org/10.1021/ie102417q>.

[17] D. Peltzer, J. Mùnera, L. Cornaglia, M. Strumendo, Characterization of potassium doped Li_2ZrO_3 based CO_2 sorbents: stability properties and CO_2 desorption kinetics, Chem. Eng. J. 336 (2018) 1–11, <https://doi.org/10.1016/j.cej.2017.10.177>.

[18] Q. Xiao, X. Tang, Y. Zhong, W. Zhu, A facile starch-assisted sol-gel method to synthesize K-doped Li_2ZrO_3 sorbents with excellent CO_2 capture properties, J. Am. Ceram. Soc. 95 (2012) 1544–1548, <https://doi.org/10.1111/j.1551-2916.2012.05090.x>.

[19] H.G. Jo, H.J. Yoon, C.H. Lee, K.B. Lee, Citrate sol-gel method for the preparation of sodium zirconate for high-temperature CO_2 sorption, Ind. Eng. Chem. Res. 55 (2016) 3833–3839, <https://doi.org/10.1021/acs.iecr.5b04915>.

[20] F. Bamiduro, G. Ji, A.P. Brown, V.A. Dupont, M. Zhao, S.J. Milne, Spray-dried sodium zirconate: a rapid absorption powder for CO_2 capture with enhanced cyclic stability, ChemSusChem 10 (2017) 2059–2067, <https://doi.org/10.1002/cssc.201700046>.

[21] B. Alcántar-Vázquez, C. Diaz, I.C. Romero-Ibarra, E. Lima, H. Pfeiffer, Structural and CO_2 chemisorption analyses on $\text{Na}_2(\text{Zr}_{1-x}\text{Al}_x)\text{O}_3$ solid solutions, J. Phys. Chem. C 117 (2013) 16483–16491, <https://doi.org/10.1021/jp4053924>.

[22] B. Dou, C. Wang, Y. Song, H. Chen, B. Jiang, M. Yang, Y. Xu, Solid sorbents for in-situ CO_2 removal during sorption-enhanced steam reforming process: a review, Renew. Sustain. Energy Rev. 53 (2016) 536–546, <https://doi.org/10.1016/j.rser.2015.08.068>.

[23] M. Shokrollahi Yancheshmeh, H.R. Radfarnia, M.C. Iliuta, High temperature CO_2 sorbents and their application for hydrogen production by sorption enhanced steam reforming process, Chem. Eng. J. 283 (2016) 420–444, <https://doi.org/10.1016/j.cej.2015.06.060>.

[24] M.Z. Memon, X. Zhao, V.S. Sikarwar, A.K. Vuppalaadityam, S.J. Milne, A.P. Brown, J. Li, M. Zhao, Alkali metal CO_2 sorbents and the resulting metal carbonates: potential for process intensification of sorption-enhanced steam reforming, Environ. Sci. Technol. 51 (2017) 12–27, <https://doi.org/10.1021/acs.est.6b04992>.

[25] K. Narasimharao, T.T. Ali, Effect of preparation conditions on structural and catalytic properties of lithium zirconate, Ceram. Int. 42 (2016) 1318–1331, <https://doi.org/10.1016/j.ceramint.2015.09.068>.

[26] N. Santiago-Torres, I.C. Romero-Ibarra, H. Pfeiffer, Sodium zirconate (Na_2ZrO_3) as a catalyst in a soybean oil transesterification reaction for biodiesel production, Fuel Process. Technol. 120 (2014) 34–39, <https://doi.org/10.1016/j.fuproc.2013.11.018>.

[27] R. Chein, C. Yu, Thermodynamic analysis of sorption-enhanced water-gas shift reaction using syngases, Int. J. Energy Res. 40 (2016) 1688–1703, <https://doi.org/10.1002/er.3554>.

[28] M.H. Halabi, J.M. De Croon, J. Van Der Schaaf, P.D. Cobden, J.C. Schouten, Reactor modeling of sorption-enhanced autothermal reforming of methane. Part I: performance study of hydrotalcite and lithium zirconate-based processes, Chem. Eng. J. 168 (2011) 872–882, <https://doi.org/10.1016/j.cej.2011.02.015>.

[29] M.H. Halabi, M.H.J.M. de Croon, J. van der Schaaf, P.D. Cobden, J.C. Schouten, Reactor modeling of sorption-enhanced autothermal reforming of methane. Part II: effect of operational parameters, Chem. Eng. J. 168 (2011) 883–888, <https://doi.org/10.1016/j.cej.2011.02.016>.

[30] B. Alcántar-Vázquez, Y. Duan, H. Pfeiffer, CO oxidation and subsequent CO_2 chemisorption on alkaline zirconates : Li_2ZrO_3 and Na_2ZrO_3 , Ind. Eng. Chem. Res. 55 (2016) 9880–9886, <https://doi.org/10.1021/acs.iecr.6b02257>.

[31] M.Z. Memon, G. Ji, J. Li, M. Zhao, Na_2ZrO_3 as an effective bifunctional catalyst-sorbent during cellulose pyrolysis, Ind. Eng. Chem. Res. 56 (2017) 3223–3230, <https://doi.org/10.1021/acs.iecr.7b00309>.

[32] D.Y. Aceves Olivas, M.R. Baray Guerrero, M.A. Escobedo Bretado, M. Marques da Silva Paula, J. Salinas Gutiérrez, V. Guzmán Velderrain, A. López Ortiz, V. Collins-Martínez, Enhanced ethanol steam reforming by CO_2 absorption using CaO^*MgO or Na_2ZrO_3 , Int. J. Hydrogen Energy 39 (2014) 16595–16607, <https://doi.org/10.1016/j.ijhydene.2014.04.156>.

[33] E. Ochoa-Fernández, H.K. Rusten, H.A. Jakobsen, M. Rønning, A. Holmen, D. Chen, Sorption enhanced hydrogen production by steam methane reforming using Li_2ZrO_3 as sorbent: sorption kinetics and reactor simulation, Catal. Today 106 (2005) 41–46, <https://doi.org/10.1016/j.cattod.2005.07.146>.

[34] J.A. Mendoza-Nieto, S. Tehuacanero-Cuapa, J. Arenas-Alatorre, H. Pfeiffer, Nickel-doped sodium zirconate catalysts for carbon dioxide storage and hydrogen production through dry methane reforming process, Appl. Catal. B Environ. 224 (2018) 80–87, <https://doi.org/10.1016/j.apcatb.2017.10.050>.

[35] C. Wang, B. Dou, B. Jiang, Y. Song, B. Du, C. Zhang, K. Wang, H. Chen, Y. Xu, Sorption-enhanced steam reforming of glycerol on Ni-based multifunctional catalysts, Int. J. Hydrogen Energy 40 (2015) 7037–7044, <https://doi.org/10.1016/j.ijhydene.2015.04.023>.

[36] J.A. Mendoza-Nieto, E. Vera, H. Pfeiffer, Methane reforming process by means of a carbonated- Na_2ZrO_3 catalyst, Chem. Lett. 45 (2016) 3–6, <https://doi.org/10.1246/cl.160136>.

[37] R. Raskar, V. Rane, A. Gaikwad, The applications of lithium zirconium silicate at high temperature for the carbon dioxide sorption and conversion to syn-gas, Water Air Soil Pollut. 224 (2013) 1569, <https://doi.org/10.1007/s11270-013-1569-2>.

[38] Y. Gao, J. Jiang, Y. Meng, F. Yan, A. Aihamaiti, A review of recent developments in hydrogen production via biogas dry reforming, Energy Convers. Manage. 171 (2018) 133–155, <https://doi.org/10.1016/j.enconman.2018.05.083>.

[39] J.-W. Kim, Y.-D. Lee, H.-G. Lee, Decomposition of Li_2CO_3 by interaction with SiO_2 in mold flux of steel continuous casting, ISIJ Int. 44 (2004) 334–341, <https://doi.org/10.2355/isijinternational.44.334>.

[40] J.-W. Kim, H.-G. Lee, Thermal and carbothermic decomposition of Na_2CO_3 and Li_2CO_3 , Metall. Mater. Trans. B 32 (2001) 17–24, <https://doi.org/10.1007/s11663-001-0003-0>.

[41] H.A. Lara-García, E. Vera, J.A. Mendoza-Nieto, J.F. Gómez-García, Y. Duan, H. Pfeiffer, Bifunctional application of lithium ferrites (Li_5FeO_4 and LiFeO_2) during carbon monoxide (CO) oxidation and chemisorption processes: A catalytic, thermogravimetric and theoretical analysis, Chem. Eng. J. 327 (2017) 783–791, <https://doi.org/10.1016/j.cej.2017.06.135>.

[42] Y. Duan, Ab initio thermodynamic approach to identify mixed solid sorbents for CO_2 capture technology, Front. Environ. Sci. 3 (2015), <https://doi.org/10.3389/fenvs.2015.00069>.

[43] S. Lowell, J.E. Shields, M.A. Thomas, M. Thommes, Characterization of Porous Solids and Powders: Surface Area, Pore Size and Density, Springer, Netherlands, Dordrecht, 2004, <https://doi.org/10.1007/978-1-4020-2303-3>.

[44] G.G. Santillán-Reyes, H. Pfeiffer, Analysis of the CO_2 capture in sodium zirconate (Na_2ZrO_3). Effect of the water vapor addition, Int. J. Greenh. Gas Control 5 (2011) 1624–1629, <https://doi.org/10.1016/j.ijggc.2011.09.009>.

[45] A. Yañez-Aulestia, J.F. Gómez-García, J.A. Mendoza-Nieto, Y. Duan, H. Pfeiffer, Thermocatalytic analysis of CO_2 - CO selective chemisorption mechanism on lithium cuprate (Li_2CuO_2) and oxygen addition effect, Thermochim. Acta 660 (2018) 144–151, <https://doi.org/10.1016/j.tca.2017.12.027>.

[46] I. Ham-Liu, J.A. Mendoza-Nieto, H. Pfeiffer, CO_2 chemisorption enhancement produced by K_2CO_3 - and Na_2CO_3 -addition on Li_2CuO_2 , J. CO₂ Util. 23 (2018), <https://doi.org/10.1016/j.jcou.2017.11.009>.

[47] A. Cruz-Hernández, J.A. Mendoza-Nieto, H. Pfeiffer, NiO- CaO materials as promising catalysts for hydrogen production through carbon dioxide capture and subsequent dry methane reforming, J. Energy Chem. 26 (2017) 942–947, <https://doi.org/10.1016/j.jechem.2017.07.002>.

[48] J. Montoya, E. Romero-Pascual, C. Gimón, P. Del Ángel, A. Monzón, Methane reforming with CO_2 over $\text{Ni}/\text{ZrO}_2\text{-CeO}_2$ catalysts prepared by sol-gel, Catal. Today 63 (2000) 71–85, [https://doi.org/10.1016/S0920-5861\(00\)00447-8](https://doi.org/10.1016/S0920-5861(00)00447-8).